# 4. Climate change and climate change scenarios

## 4.1 Introduction

The Intergovernmental Panel for Climate Change (IPCC) released its Fourth Assessment Report (AR4) in April 2007. It found that "*Warming of the climate system is unequivocal, as is now evident from observations of increases in global average air and ocean temperatures, widespread melting of snow and ice, and rising global mean sea level*".

The IPCC was formed in 1988 to provide reliable scientific advice on climate change. Approximately every six years it has produced a full assessment of the current state of scientific knowledge on climate change and what it means for us. The reports synthesise evidence and analysis published either in peer-reviewed scientific journals or other credible sources. It latest report involved over 1200 scientific authors and 2500 expert reviewers from more than 130 countries.

To assess how the global climate may change in the future, projections are made using computer models of the earth's climate. These Global Climate Models (GCMs) simulate the effect on the atmosphere and oceans of different possible future scenarios of greenhouse gas emissions. A range of possible future emission scenarios (40 in total) have been defined by the IPCC as we do not know exactly how much greenhouse gases will be emitted over the coming century, and therefore can not define exactly how this will translate into climate changes. For the Fourth Assessment Report the focus was on six scenarios (known as the emission marker scenarios, individually termed B1, A1T, B2, A1B, A2 and A1FI), which spanned the full range of all IPCC emission scenarios, Table 8.

The GCM's and the emission scenarios represent the two major sources of uncertainty in projecting how the climate may change in the future:

- The sensitivity of the global climate models to changes in carbon dioxide varies, i.e., some models suggest a greater increase in surface temperatures (and hence other climate and ocean parameters) than others to the same increase in greenhouse gas concentrations.

- Future emissions of greenhouse gases are not certain as they depend on factors such as population changes, economic growth, technology, energy use, national and international policies.

It is largely due to these uncertainties that projections of future changes in temperature, sea-level rise etc. are presented as a range, rather than a single value. The IPCC does not give any indication whether any one emission scenario is more likely than another, hence in this report we consider the full range of emission scenarios. However, the scenario labelled "A1B", which gives an intermediate level of warming by the end of the century, has more GCM output data available than any other scenario.

**Table 8:** Summary of emission scenarios used in the IPCC AR4.

| Scenario | Description of emission | Approximate carbon dioxide stabilisation scenario |
|---|---|---|
| **A1FI** | High end of the scenarios range | Does not stabilise |
| **A1B** | Intermediate case (middle-of-the-road scenario) | 750 ppm |
| **A1T** | Intermediate/low case | 650 ppm |
| **A2** | High case | Does not stabilise |
| **B1** | Low end of the scenario range | 550 ppm |
| **B2** | Intermediate/low case | 650 ppm |

## 4.2 Future sea-level rise

### 4.2.1 IPCC Forth Assessment Report

Sea levels will continue to rise over the 21st century and beyond, primarily because of thermal expansion within the oceans and loss of ice sheets and glaciers on land. The basic range of projected global sea-level rise estimated in the AR4 is for a rise of 0.18 m to 0.59 m by the decade 2090-2099 (mid 2090s) relative to the average sea level over the period 1980 to 1999, Figure 16. This is based on projections from 17 different Global Climate Models (GCMs) for the six different future emission scenarios mentioned above. The ranges for each emission scenario are 5 to 95% intervals characterising the spread of GCM results (bars on the right-hand side of Figure 7). However, these projections exclude uncertainties in carbon cycle feedbacks and the possibility of faster ice melt from Greenland and West Antarctica ice sheets.

The basic set of projections (light blue shading in Figure 16) include sea-level contributions due to changes in surface mass balance of the polar ice sheets (Greenland and Antarctica) at the rates observed between 1993 to 2003. It did not include the contributions due to changes in the dynamics of ice-sheet discharge (which

is less well understood and likely to be an increasing factor particularly if greenhouse gas emissions are not reduced). IPCC (2007a) provides an estimated rise in the upper ranges of the emission scenario projections (dark blue shading) that would be expected with "scaled-up ice sheet discharge" if contributions to sea-level rise were to grow linearly with global temperature change for each emission scenario. This was estimated within the IPCC AR4 as varying between an additional 0.09 m to 0.17 m (depending on emission scenario) but was rounded up in the IPCC summary reports to an additional 0.1 to 0.2 m rise. This potential future contribution to sea–level rise from increased ice-sheet discharge from Greenland and West Antarctic is a major source of uncertainty, with the physical processes relatively poorly understood (and hence not well represented in existing GCM's). Hence IPCC AR4 also concluded that a larger contribution from these ice sheets, especially from Greenland, over this century could not be ruled out (see further information below).

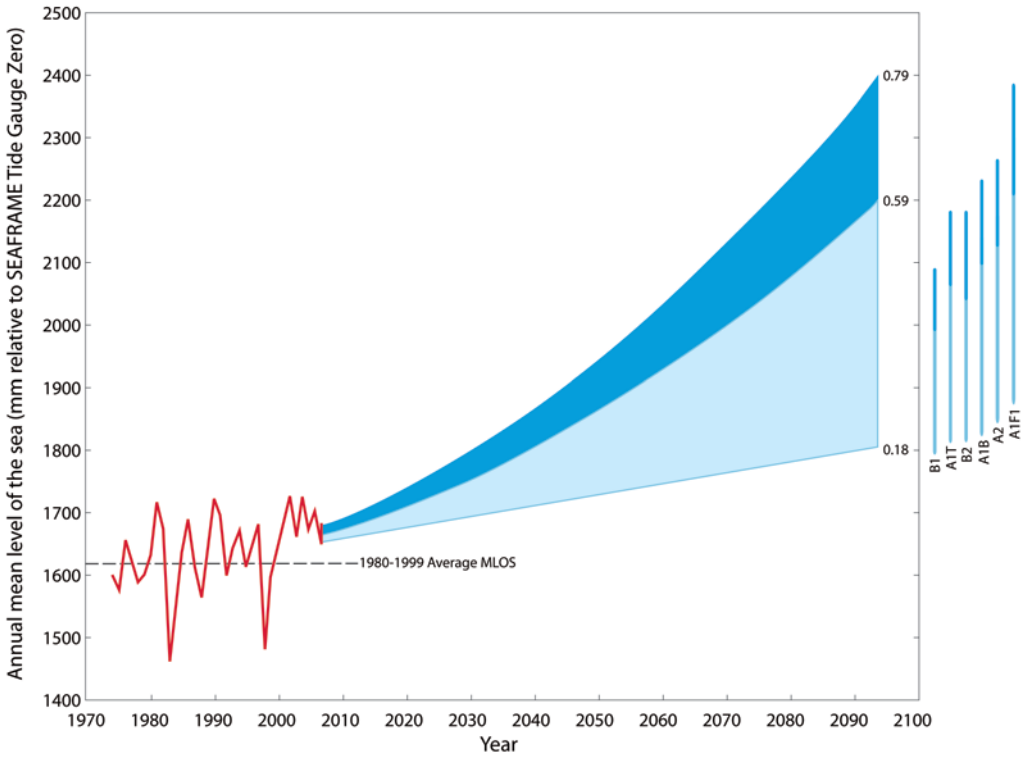


**Figure 16:** Global mean sea-level rise projections to the mid 2090s in the context of historical mean annual sea-level measurements at Tarawa back to 1974. The red line is the annual mean level of the sea as measured by the various sea-level gauges at Tarawa between 1974 and 2007. The light blue shading shows the range in projected mean sea level out to the 2090's for the six emission marker scenarios. The dark blue shading shows the potential additional contribution of up to 0.2 m from Greenland and West Antarctica Ice Sheets due to scaled-up ice sheet discharge. The vertical colour lines on the right-hand side show the range in projections from the various GCM's for six emission scenarios, with the dark blue line above each, the potential additional scaled up ice-sheet discharge for each scenario.

In addition to the uncertainties of the future rate of global sea-level discussed above, we also need to consider whether global projections of sea-level rise are representative of the Kiribati region. This depends on:

1. Departures (positive or negative) from the global average in different sub-regions of the world's oceans. Examples are differences due to non-uniform patterns of temperature and salinity change, variations in mean surface atmospheric pressure and wind stress, and varying response of ocean current circulation to climate change. As yet these geographical variations are poorly understood but they can be significant. An assessment of the various GCM output for the A1B scenario within the IPCC AR4 suggests that long-term sea-level change in the Kiribati region will be relatively close (within ±0.05 m over 100 years) to the global average, Figure 17.

2. Local vertical land movements. The landmass can either be stable, subsiding or rising. In the case of Kiribati, the overall landmass movements are likely to be insignificant when compared with sea-level rise rates over the timeframes of interest, i.e., 100 years.

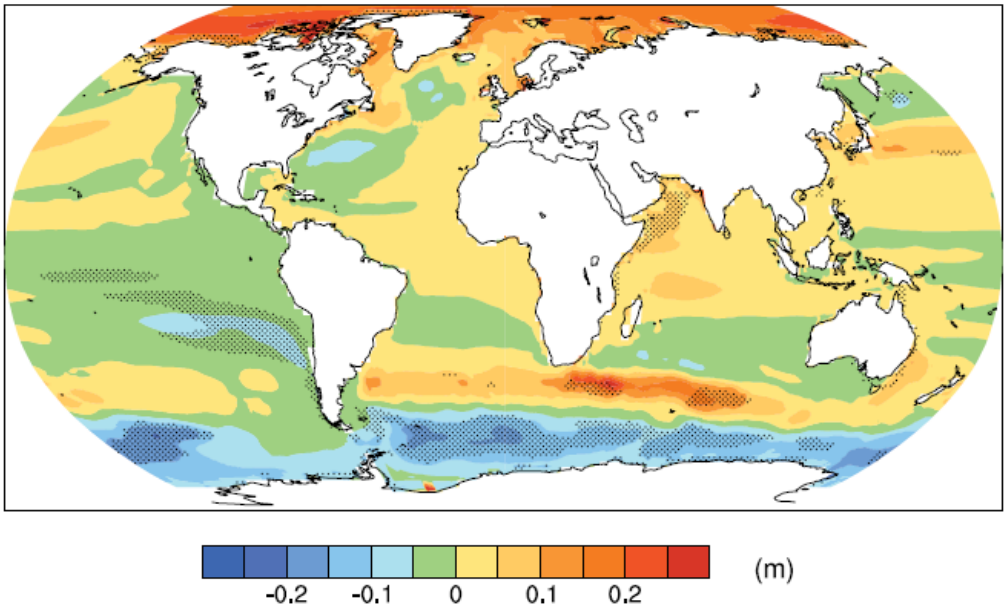


**Figure 17:** Regional sea level change due to density and circulation change relative to the global average (i.e., +ve values indicate greater regional sea level than the global average) during the 21st century. These changes have been calculated as the difference between average for 2080 to 2099 and 1980 to 1999, as an ensemble mean over 16 climate-ocean circulation models for the SRES A1B scenario (IPCC, 2007a).

### 4.2.2 Science literature since the Fourth Assessment Report

Since the cut-off point for science publications to be considered within the IPCC Fourth Assessment Report process, further scientific papers have been published. These add to the array of information on potential future sea-level rise over this century and include:

- Carbon dioxide emissions have been growing about four times faster since 2000 than during the previous decade, despite efforts to reduce emissions in a number of the Kyoto Protocol signatory countries. Between 2000 and 2007 global emissions growth was above that of the most fossil fuel intensive emission (A1FI) scenario of the IPCC (Global Carbon Project, 2008).

- Confirmation that the Antarctic ice cap is shrinking (i.e., losing mass), Rignot et al. (2008, Shepherd and Wingham (2007), Bamber et al. (2007). However, it is as yet unclear whether this trend of increased discharge of ice from Antarctica is a response to recent climate change and will continue into the future, or whether it is a rapid short-term adjustment that will reduce in the near future.

- Glaciological conditions required for a sea-level rise of above 2 m by 2100 are unlikely to occur (Pfeffer et al. 2008). They suggest that a "most likely" starting point for refining sea-level rise to 2100 including increased ice dynamics lies between 0.8 and 2 m. However, they emphasises that there are still considerable uncertainties and assumptions made.

- Higher estimates of sea-level rise over the 21st century than suggested by the IPCC Fourth Assessment Report are also the conclusion from a number of other more recent studies (Rahmstorf, 2007; Horton et al. 2008; Grinsted et al. 2010'; Vermeer and Rahmstorf, 2009; Jevrejeva, 2010). The ranges of sea-level rise estimates by 2100 or 2090s (2090-2099) are summarised in Figure 18.

  However, the methodology used in these studies was relatively simplistic based on a derived relationship between changes in global near-surface temperatures and sea level. As yet no scientific consensus has been reached over the validity of this methodology.

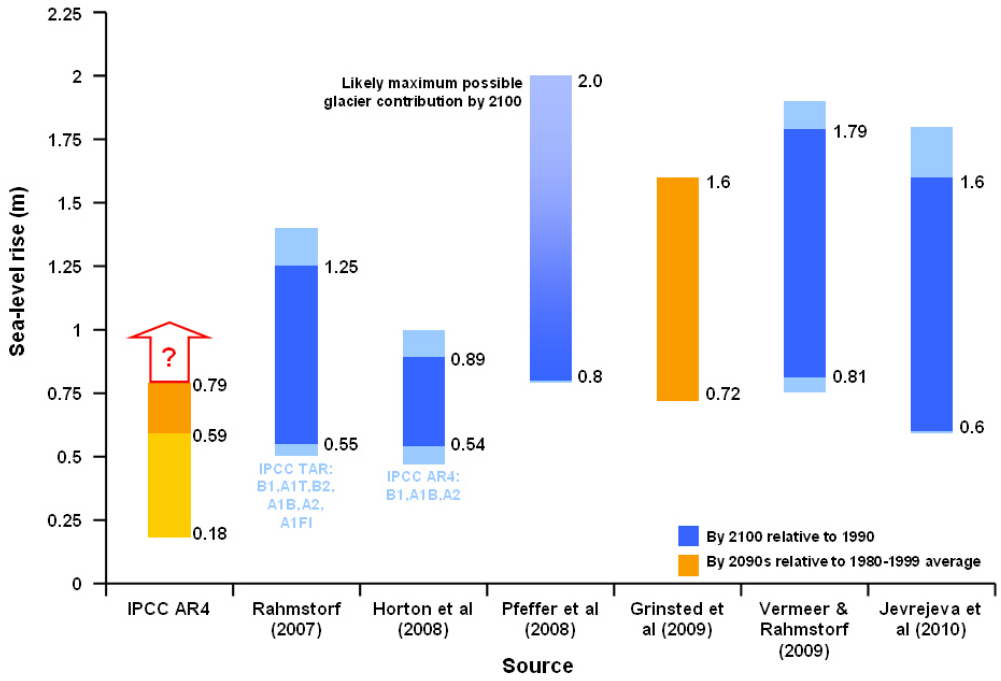


**Figure 18:** Summary of sea-level rise estimates from recent science publications. The dark blue bars show the range in projection for the various emission scenarios used. The light blue bars show the upper and lower error margins.

### 4.2.3 Sea-level rise guidance for Kiribati

The IPCC Fourth Assessment Report found that "Because the understanding of some of the important effects driving sea-level rise is too limited, this report does not assess the likelihood, nor provide a best estimate or an upper bound of sea-level rise". As such, and given the issues and uncertainties discussed above, it is not possible to define "one" definitive (or "most likely") sea-level rise rate to be used in assessments where sea-level rise needs to be considered.

It is important that where such uncertainty does exist that a full understanding of the sensitivity of the decision or issue under consideration to potential different sea-level rise rates is developed (i.e., what impact does a different sea-level rise than the one assumed have on my decision or issue under consideration?).

Based on a discussion of the above, three future timeframes that were representative for I-Kiribati decision-making, and three future climate change scenarios, were selected by the I-Kiribati participants to be used for routine climate change assessments (Tables 9 and 10). The decision was made to focus on the IPCC AR4 scenarios over the three timeframes, rather than accommodate higher sea-level

magnitudes on the basis that the global community does agree and implement mitigation measures that limits the upper projections of sea-level rise being suggested in Section 4.2.2 over this century. Figure 19 shows the three future sea-level trends superimposed on to the 1974 to 2008 annual mean sea-level record measured at Betio.

**Table 9:** I-Kiribati selected climate change scenarios

| Scenario | Description |
|---|---|
| **Low:** IPCC Scenario B2 | Low range of model output (5%) + no scaled-up ice sheet component by 2090) |
| **Intermediate:** IPCC Scenario A2 | Mid range of model output (50%) + 10 cm scaled up ice sheet component by 2090 |
| **High:** IPCC Scenario A1FI | Upper range of model output (95%) + 20 cm scaled up ice sheet component by 2090. |

**Table 10:** I-Kiribati timeframes for general climate change assessment and sea-level rise magnitudes for the three climate change scenarios (relative to the 1980-1999).

| Timeframe Name (English) | Timeframe Name (I-Kiribati) | Timeframe | Climate change scenario | | |
|---|---|---|---|---|---|
| | | | Low | Intermediate | High |
| | | | SLR (m) | SLR (m) | SLR (m) |
| Grand children | Te tibu | 2012 - 2036 | 0.09 | 0.13 | 0.20 |
| Great-grand children | Tibu-toru | 2036 - 2060 | 0.13 | 0.22 | 0.35 |
| Great-great grand children | Tibu-mwamwanu | 2060 - 2084 | 0.17 | 0.33 | 0.55 |

### 4.2.4 Comparison with sea-level rise allowances in the existing Climate Change Adaptation Strategy

The present Climate Change Adaptation Strategy (CCAS), (Government of Kiribati, 2005), assumes a sea-level rise for 2025, 2050 and 2100 of +6 cm (+3 cm to + 10 cm), +14 cm (+6 cm to + 26 cm) and +39 cm (+12 cm to +83 cm), respectively relative to the year 2000. These values are based on four emission scenarios and the results from three climate models. Figure 20 summarises how these values compare with sea-level rise magnitudes and timeframes presented in the previous sections.

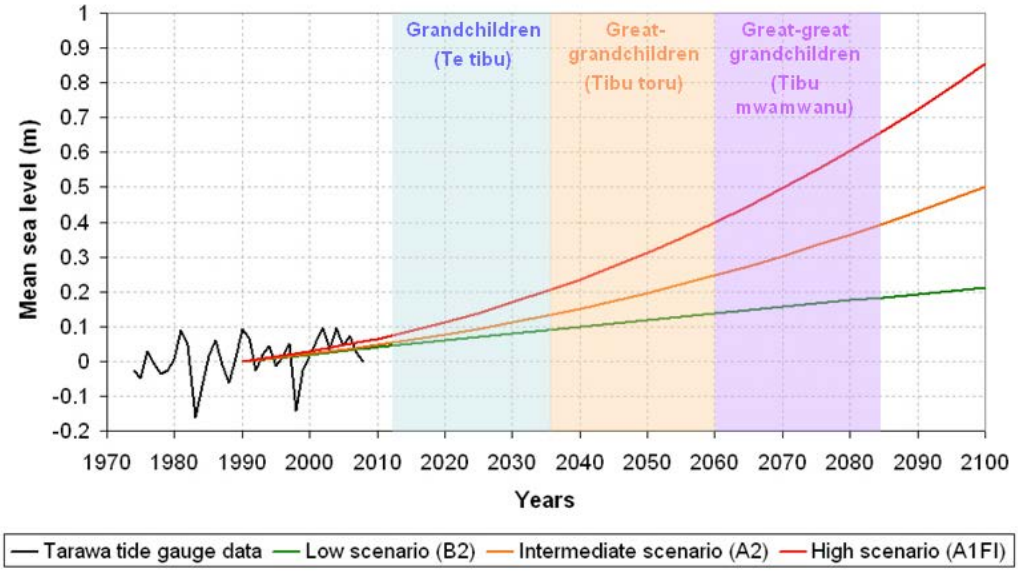


**Figure 19:** Mean annual sea levels measured by the various Tarawa tide gauges relative to 1980-1999 average with mean sea-level rise for the three I-Kiribati climate change scenarios.

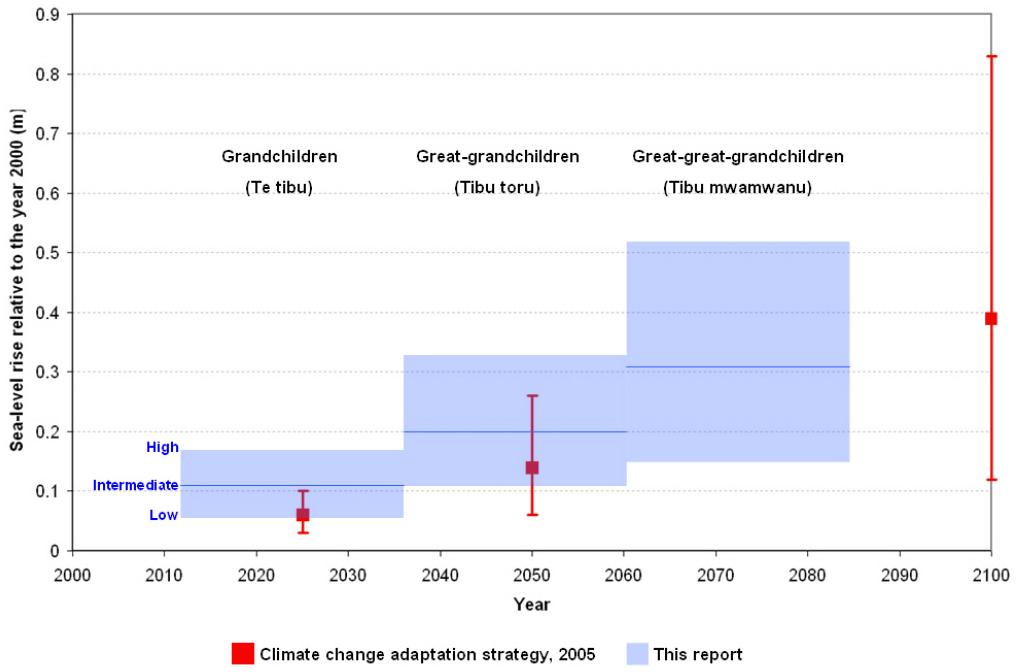


**Figure 20:** Comparison between sea-level rise allowance within the current Climate Change Adaptation Strategy (2005) and the suggested allowance within this report. All sea-level rise values have been adjusted to the year 2000 based on the difference in mean level of the sea at Tarawa between the 1980-1999 average and 2000.

## 4.3 Magnitude of future sea-level rise relative to present day high tide levels

Deep-ocean tide ranges will not be directly affected by climate change. However, with rising sea levels the frequency of high tides exceeding a given land level will change depending on the size of tide range. Problems are likely to be greater for locations with smaller tide ranges in relation to sea-level rise, where future high tides will more often exceed current upper-tide levels.

For each island we have derived a high-tide exceedance curve from tide predictions over the next 100 years[2]. These exceedence curves provide the frequency at which a given astronomical high tide is exceeded over this time period (i.e., excluding sea-level rise and climate / meteorological variability). Figure 21 shows the high-tide exceedance curves for Tarawa, Kanton Island and Kiritimati, with similar plots for the other Western Kiribati islands contained in Appendix 5.

The exceedance curves are provided in terms of high tide above present day Mean Level of the Sea (MLOS). In the case of Tarawa, to translate the values on this curve to an elevation relative to the SEAFRAME Gauge 0 datum, MLOS needs to be added to the curve (for example the average MLOS over 2007 was 1.637 m above SEAFRAME Gauge 0).

The plots in Figure 21 also show the same high-tide exceedance curve but with sea level rises added on of 0.18 m (green), 0.59 m (blue) and 0.79 m (red) representing the 5% and 95% IPCC range in sea level by the 2090s for the six emission marker scenarios (see Section 4.1), and the potential upper additional contribution due to increased ice melt, respectively.

If we consider the present day Mean High Water Perigean Spring (MHWPS) level and shown as one of the horizontal grey lines in the plots), at Tarawa, this is exceeded by about 15% of all high tides at present. For a 0.18 m rise in sea-level, present-day MHWPS levels would be exceeded by about 29% of all high tides, and for a 0.59 m and 0.79 m rise by 76% and 96% of all high tides respectively. These changes are generally similar for all the other western Kiribati islands.

However, for Kanton Island, and more so Kiritimati, where the tide range is much smaller, future sea-level rise has a much more significant influence. For Kanton Island, virtually all high tides (99%) will exceed present-day MHWPS levels under a

[2] The tide predictions for each island are based on eight harmonic constituents for each island location derived from the global tide model of Andersen (2006), with the exception of Tarawa where a full harmonic analysis of the University of Hawaii and SEAFRAME sea-level datasets was undertaken.

0.59 m rise in sea level. For Kiritimati, a sea-level rise of 0.18 m (the lowest range of the IPCC projections by the 2090s) results in 85% of high tides exceeding present-day king tide levels. For a sea-level rise of 0.59 m all high tides will exceed present-day king tide levels by at least 0.28 m, and for a sea-level rise of 0.79 m by at least 0.48 m.

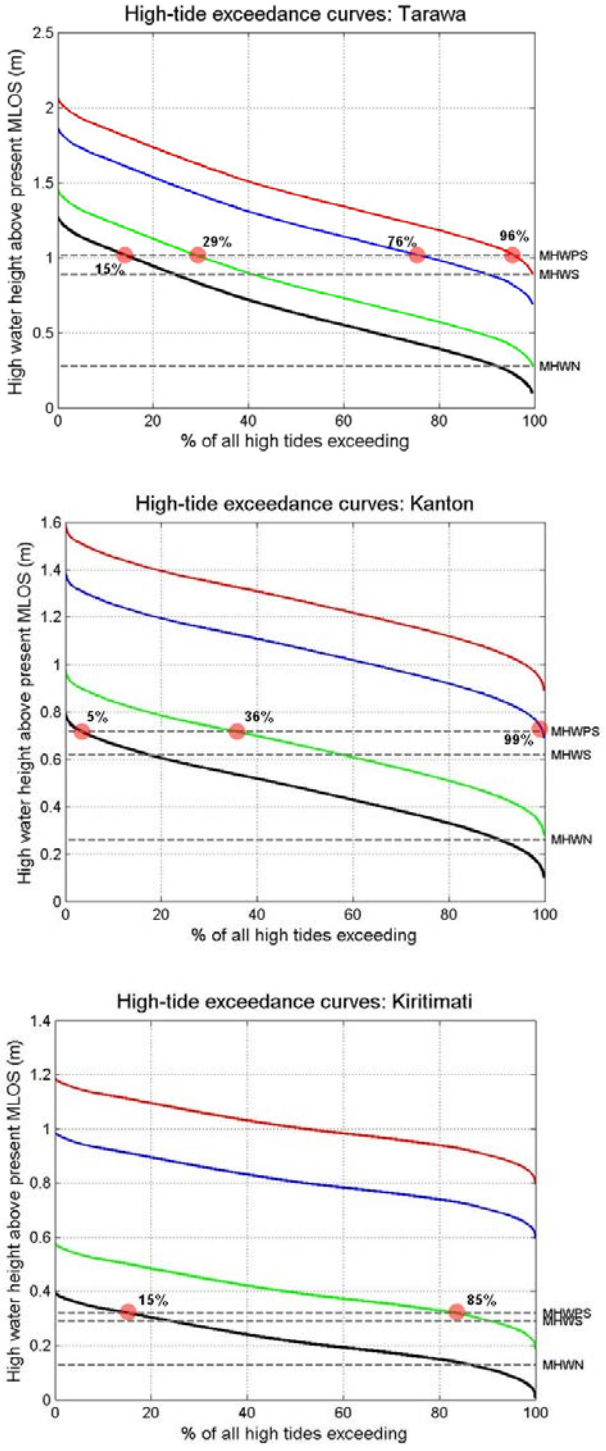


**Figure 21:** High-tide exceedance curves based on a simulation of 100 years of tides at Tarawa (top), Kanton Island (middle) and Kiritimati (bottom) for the present day relative to Mean Level of the Sea (MLOS) and for a 0.18 m (green), 0.59 m (blue) and 0.79 m (green) rise in sea level. Also shown are the present day Mean High Water Neap (MHWN), Mean High Water Spring (MHWS) and Mean High Water Perigean Spring (MHWPS) levels (grey dashed lines).

## 4.4 Climate change effects on other hazard drivers

There has been little progress since the Third Assessment Report in 2001 in understanding the effects climate change is having, and will have, on the other drivers of coastal hazards, such as storms, storm surge, waves and swell.

Global climate models are presently most suited for considering changes in large-scale dynamics of the atmosphere-ocean system. Whilst the GCM's can provide indications of general changes in phenomena (e.g., mean winds, pressure, rainfall, etc.) they are not suited to assessing variability and change in more transient phenomena such as intense storms. Hence, there is still much uncertainty as to potential changes to the more extreme conditions (which is the focus of this assessment).

From the viewpoint of coastal flood and erosion hazards, of potentially greater concern than a rise in mean sea level is any change in the magnitude or frequency of storm-tide levels or changes in extreme wave conditions that affect the magnitude or occurrence of wave set-up (and hence wave translation over the fringing reef, run-up and overtopping).

Globally, there have been few studies of long-term changes in extreme sea levels. Most of the studies that have been conducted have found considerable variation from year to year associated with periods of increased storminess but little evidence (yet) for an increase in storm tide levels relative to the underlying upward trend in mean sea level.

Changes in storm surge and wave heights (discussed in the next section), are only beginning to be assessed within a few of the GCM's (mainly related to cyclone changes) with there being insufficient certainty yet to reliably quantify how storm surge and wave conditions may change. For extreme significant wave heights an indicative change is provided by Caires et al. (2006) which suggested for three emission scenarios that the 20-year (i.e., 5% AEP) significant wave heights in the Kiribati region could vary by up to ±10% depending on season and location. But, given the limitations in the GCM's that were used to drive the global wave model, such results should be treated with caution.

Furthermore, in Kiribati, as in much of the Pacific, both sea levels and wave climate are significantly influenced by ENSO phase. Whilst there has been significant progress in understanding and representing ENSO characteristics within the GCM's there still remain some significant deficiencies, including adequately representing the sea surface temperature gradient along the equator. Whilst most of the GCM models

do indicate an increase in El Niño like conditions (which would suggest an increase in westerly wave conditions), a number suggest the opposite.

As a result, there is little in the IPCC AR4 to reliably quantify how extreme storm surge and ocean wave conditions may change around Kiribati. Until any such information on potential changes is available, the following is suggested for practical coastal-related assessments:

- Astronomic tide characteristics do not change from those at present.
- Storm surge height characteristics do not change from those at the present.
- The sensitivity of wave height change on the particular issue under consideration be assessed by varying extreme wave heights by ±5%.

Based on these assumptions, the same hydrodynamic model of Tarawa lagoon, described in Section 3.2.6 was used to assess variability in storm-tide levels around the lagoon shoreline under sea level rise conditions, Figure 22.

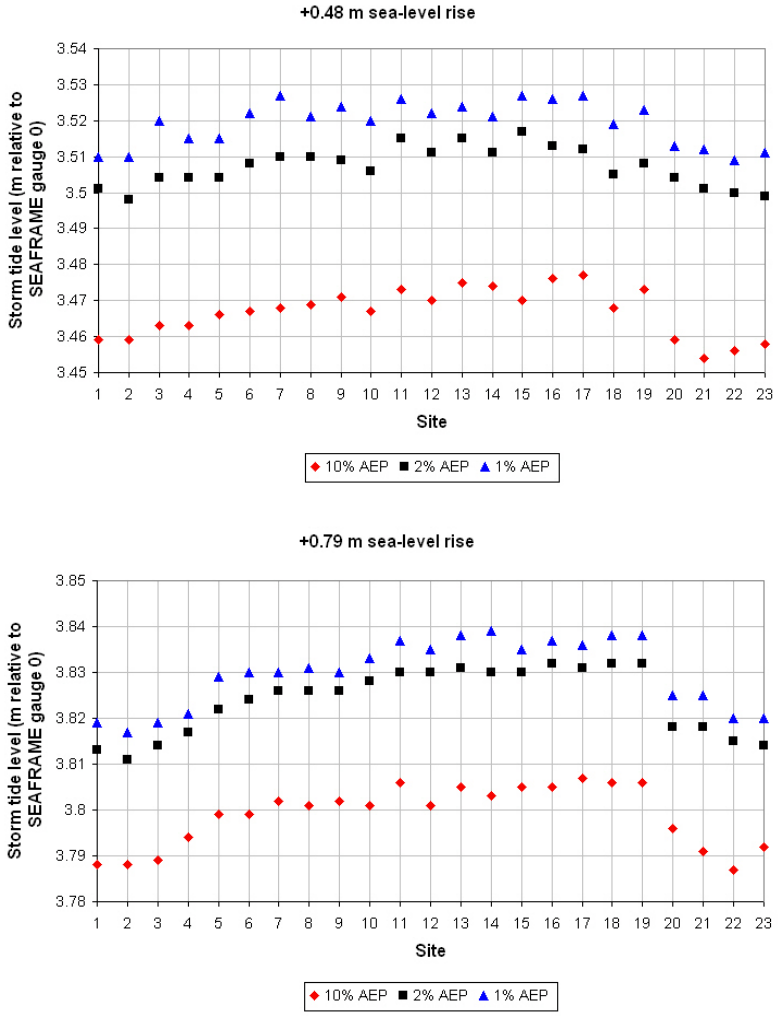


**Figure 22:** 10%, 2% and 1% Annual Exceedance Probability (AEP) storm tide levels (relative to SEAFRAME Gauge 0) at the 23 representative locations around Tarawa lagoon for a 0.48 m rise in sea level (top) and 0.79 m rise in sea-level (bottom).

# 5. Ocean shoreline wave conditions

## 5.1 Deepwater wave conditions

Around each atoll shoreline a deepwater wave climate based on the NOAA/NCEP Wavewatch hindcast for the period 1 February 1997 to 1 November 2007 was derived (Figure 23).

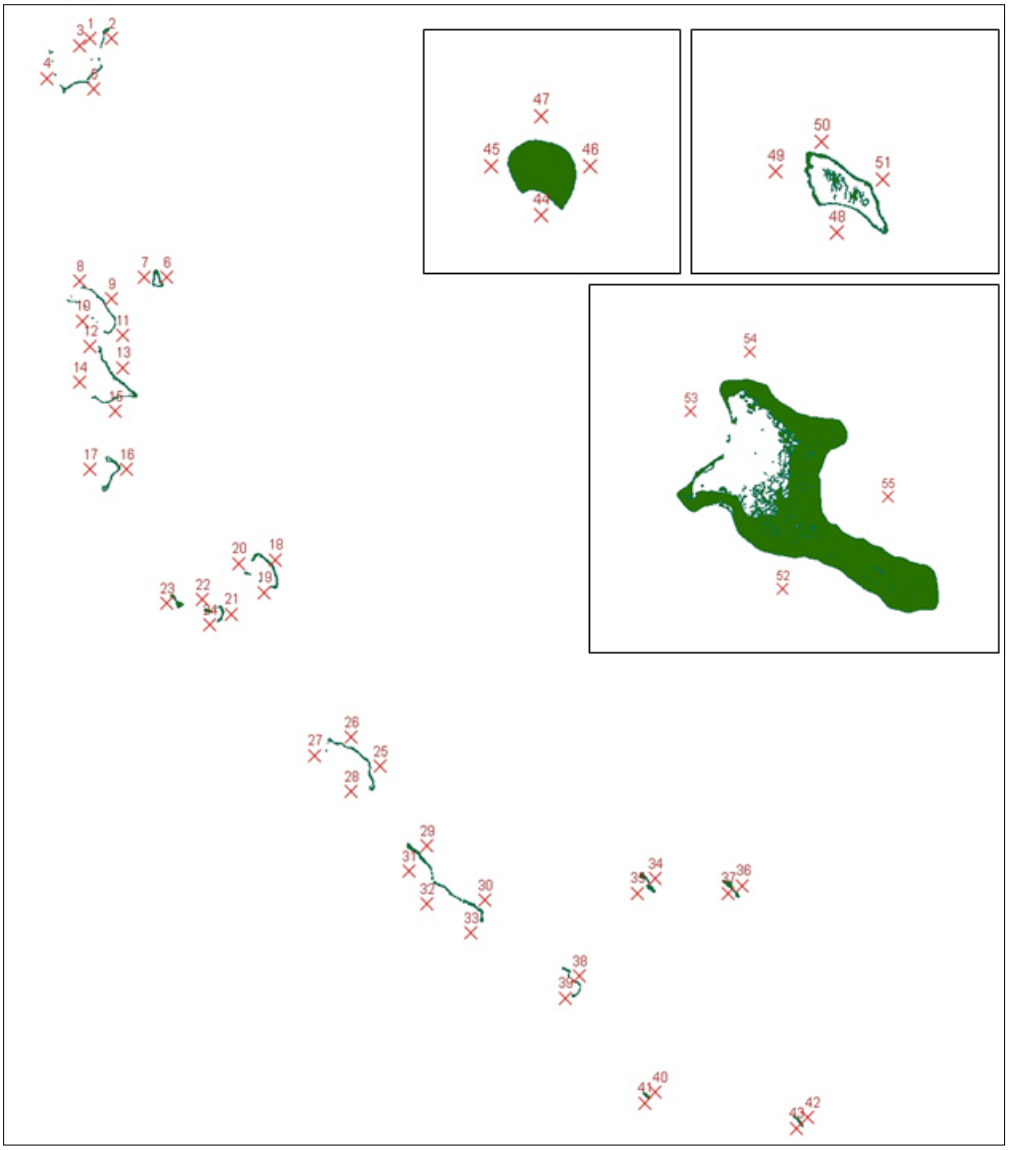


**Figure 23:** Locations around each of the western Kiribati Islands where offshore wave climate data and extreme wave conditions have been derived. The insets show the wave climate and extreme data locations around Banaba, Kanton and Kiritimati.

Wave statistics were interpolated from the NOAA/NCEP grid (at a resolution of 1.25º in longitude, 1.0º in latitude) to the output locations using a method that accounts for the sheltering effect of each wave direction by atoll landmass.

Based on the wave climate at each location, 10%, 2% and 1% deep-water significant wave height Annual Exceedance Probabilities (and their corresponding peak and mean wave periods) were derived based on the methodology summarised in Appendix 3 (Section 13.2.1). These significant wave heights are summarised in Table 11.

**Table 11:** Summary of 10%, 2% and 1% AEP offshore significant wave heights around various islands in Kiribati.

| Site | Location | Longitude | Latitude | Extreme offshore significant wave height (m) | | |
|---|---|---|---|---|---|---|
| | | | | 10 yr 10% AEP | 50 yr 2% AEP | 100 yr 1%AEP |
| 1 | Makin (West) | 172.9127 | 3.34 | 3.21 | 3.36 | 3.41 |
| 2 | Makin (East) | 173.0329 | 3.34 | 3.67 | 3.91 | 4.00 |
| 3 | Butaritari (North) | 172.8526 | 3.3 | 3.32 | 3.53 | 3.61 |
| 4 | Butaritari (West) | 172.6723 | 3.12 | 2.97 | 3.27 | 3.38 |
| 5 | Butaritari (South-East) | 172.9327 | 3.06 | 3.57 | 3.79 | 3.87 |
| 6 | Marakei (East) | 173.3333 | 2.02 | 3.05 | 3.28 | 3.38 |
| 7 | Marakei (West) | 173.2131 | 2.02 | 3.06 | 3.23 | 3.29 |
| 8 | Abaiang (North) | 172.8526 | 2 | 3.40 | 3.91 | 4.16 |
| 9 | Abaiang (East) | 173.0329 | 1.9 | 3.25 | 3.68 | 3.89 |
| 10 | Abaiang (South-West) | 172.8726 | 1.78 | 3.04 | 3.80 | 4.14 |
| 11 | Abaiang (South-East) | 173.0929 | 1.7 | 3.16 | 3.32 | 3.38 |
| 12 | Tarawa (North) | 172.9127 | 1.64 | 3.09 | 4.30 | 5.04 |
| 13 | Tarawa (East) | 173.0929 | 1.52 | 3.18 | 3.36 | 3.43 |
| 14 | Tarawa (West) | 172.8526 | 1.44 | 3.06 | 3.76 | 4.10 |
| 15 | Tarawa (South) | 173.0529 | 1.28 | 2.70 | 3.06 | 3.22 |
| 16 | Maiana (East) | 173.113 | 0.96 | 3.16 | 3.46 | 3.59 |
| 17 | Maiana (West) | 172.9127 | 0.96 | 3.14 | 3.69 | 3.96 |
| 18 | Abemama (East) | 173.9343 | 0.46 | 3.38 | 3.74 | 3.90 |
| 19 | Abemama (South) | 173.8742 | 0.28 | 3.04 | 3.78 | 4.20 |
| 20 | Abemama (West) | 173.734 | 0.44 | 3.37 | 3.71 | 3.85 |
| 21 | Aranuka (East) | 173.6939 | 0.16 | 3.21 | 3.47 | 3.58 |
| 22 | Aranuka (North) | 173.5337 | 0.24 | 3.22 | 3.47 | 3.57 |
| 23 | Kuria (West) | 173.3333 | 0.22 | 3.24 | 3.80 | 4.06 |
| 24 | Aranuka/Kuria (South) | 173.5737 | 0.1 | 3.18 | 4.19 | 4.78 |
| 25 | Nonouti (East) | 174.5152 | -0.68 | 3.19 | 3.37 | 3.43 |
| 26 | Nonouti (North-East) | 174.355 | -0.52 | 3.39 | 3.70 | 3.83 |
| 27 | Nonouti (West) | 174.1546 | -0.62 | 3.14 | 3.64 | 3.86 |

| Site | Location | Longitude | Latitude | Extreme offshore significant wave height (m) | | |
|---|---|---|---|---|---|---|
| | | | | 10 yr 10% AEP | 50 yr 2% AEP | 100 yr 1%AEP |
| 28 | Nonouti (South-West) | 174.355 | -0.82 | 3.01 | 3.46 | 3.65 |
| 29 | Tabiteuea (North-East) | 174.7756 | -1.12 | 3.01 | 3.23 | 3.33 |
| 30 | Tabiteuea (East) | 175.0962 | -1.42 | 3.25 | 3.54 | 3.66 |
| 31 | Tabiteuea (North-West) | 174.6755 | -1.26 | 3.09 | 3.35 | 3.45 |
| 32 | Tabiteuea (West) | 174.7756 | -1.44 | 3.07 | 3.35 | 3.45 |
| 33 | Tabiteuea (South) | 175.016 | -1.6 | 3.07 | 3.45 | 3.62 |
| 34 | Beru (East) | 176.0377 | -1.3 | 3.23 | 3.33 | 3.36 |
| 35 | Beru (West) | 175.9375 | -1.38 | 3.02 | 3.36 | 3.49 |
| 36 | Nikunau (East) | 176.5184 | -1.34 | 3.38 | 3.66 | 3.77 |
| 37 | Nikunau (West) | 176.4383 | -1.38 | 3.15 | 3.53 | 3.68 |
| 38 | Onotoa (East) | 175.617 | -1.84 | 3.11 | 3.29 | 3.35 |
| 39 | Onotoa (West) | 175.5369 | -1.96 | 3.32 | 3.91 | 4.20 |
| 40 | Tamana (East) | 176.0377 | -2.48 | 3.44 | 3.68 | 3.76 |
| 41 | Tamana (West) | 175.9776 | -2.54 | 3.60 | 4.22 | 4.52 |
| 42 | Arorae (East) | 176.879 | -2.62 | 3.53 | 3.94 | 4.12 |
| 43 | Arorae (West) | 176.8189 | -2.68 | 3.73 | 4.61 | 5.05 |
| 44 | Banaba (South) | 169.535 | -0.875 | 3.34 | 3.74 | 3.90 |
| 45 | Banaba (West) | 169.515 | -0.855 | 3.44 | 3.89 | 4.08 |
| 46 | Banaba (East) | 169.555 | -0.855 | 2.86 | 3.07 | 3.16 |
| 47 | Banaba (North) | 169.535 | -0.835 | 3.25 | 3.76 | 4.01 |
| 48 | Kanton (South) | 188.32 | -2.87 | 3.71 | 4.60 | 5.07 |
| 49 | Kanton (West) | 188.24 | -2.79 | 4.03 | 4.43 | 4.59 |
| 50 | Kanton (North) | 188.3 | -2.75 | 4.13 | 4.47 | 4.60 |
| 51 | Kanton (East) | 188.38 | -2.8 | 3.69 | 3.79 | 3.81 |
| 52 | Kiritimati (south) | 202.6 | 1.73 | 3.56 | 3.94 | 4.12 |
| 53 | Kiritimati (West) | 202.46 | 2 | 4.17 | 4.27 | 4.30 |
| 54 | Kiritimati (North) | 202.55 | 2.09 | 4.25 | 4.34 | 4.36 |
| 55 | Kiritimati (East) | 202.76 | 1.87 | 3.73 | 3.95 | 4.03 |

Larger swell conditions are known to have occasionally affected Kiribati and other South Pacific islands in the past. For example, Matthews (1971) described damage on northern shorelines of a number of Pacific Islands in early December 1969 due to two storms in the North Pacific (between 40ºN and 50ºN), with the resulting swell waves travelling over 7000 km to the south. Large swell between 4 m and 6 m high affected the northern coasts of islands in Kiribati (noted at Butaritari, Tarawa, Beru, Arorae and Kiritimati), Tuvalu, Samoa, Cook Islands and Tahiti. A similar event affected the northern coats of Marakei during December 2008 caused by a storm event to the northwest which resulted in large swell propagating to the south.

The accuracy of the estimated extreme wave heights from a dataset is limited by the length of dataset available. The 10 years of data available from the Wavewatch hindcast dataset would generally be considered the very minimum length of dataset required to derive annual exceedance probability wave heights of 1% and as such may slightly under predict such wave heights if similar events such as the one noted above did not occur during the last 10 years. Furthermore, wave forecast/hindcast models often under-predict the largest wave heights during storms, mainly because the wind fields fed to them are time-averaged and so the energy transfer from strong wind gusts to wave growth is absent (e.g., Stephens & Gorman, 2006). For Kiribati, given its location close to the equator and lack of tropical cyclones or significant low-pressure storm systems, this may not be as significant an issue as in other locations.

## 5.2 Wave set-up and wave height translation over fringing ocean reefs

### 5.2.1 Wave set-up

Waves breaking on the edge of the ocean-side fringing reef around the various atolls and islands in Kiribati result in water being "pumped" over the reef. This causes an increase in sea level (known as wave set-up) over the reef flat, which in turn can allow larger than normal waves to translate over the reef flat and reach the shoreline, causing increased wave run-up, overtopping and overwashing (see Figure 1 & 24).

On Kiribati, after the influence of astronomical tide, wave set-up on the fringing reefs is usually the most significant factor raising sea levels over reef flats; in some cases, such set-up can be half the offshore wave height. Wave breaking, wave set-up, the transformation of waves and wave-induced flows over the reef to the shoreline is a complex process and still relatively poorly understood. However, it is heavily influenced by:

- The shape of the reef profile, permeability and roughness of the reef, and how these vary along the coast.

- Wave height and period, with the magnitude of wave set-up tending to increase with increased wave height and period.

- Tide level and any storm surge (i.e., storm-tide level), with increasing influence exerted by the reef-top topography as the depth of water over the reef flat decreases (wave set-up magnitude generally decreases with increasing water depth over the reef).

Furthermore, wave set-up can vary considerably over short timescales due to the influence of wave grouping. Large waves in a wave group discharge a greater than average volume of water on to the reef-top (Gourlay, 1996), increasing the wave set-up, and allowing larger waves to translate over the reef flat to the shoreline. After these large waves have passed, the smaller waves following cannot sustain this set-up, and water flows back seawards over the reef edge, particularly through any lower lying sections of the reef (e.g., reef channels). This seaward flow steepens the smaller waves, causing them to break more fully, resulting in much smaller waves translating over the reef flat to the shore. The process is repeated when the next group of large waves breaks on the reef edge. This dynamic fluctuation in reef top set-up (known as surf beat) varies with the timing of the wave groups (hence the largest waves often occur at four to five minute intervals).

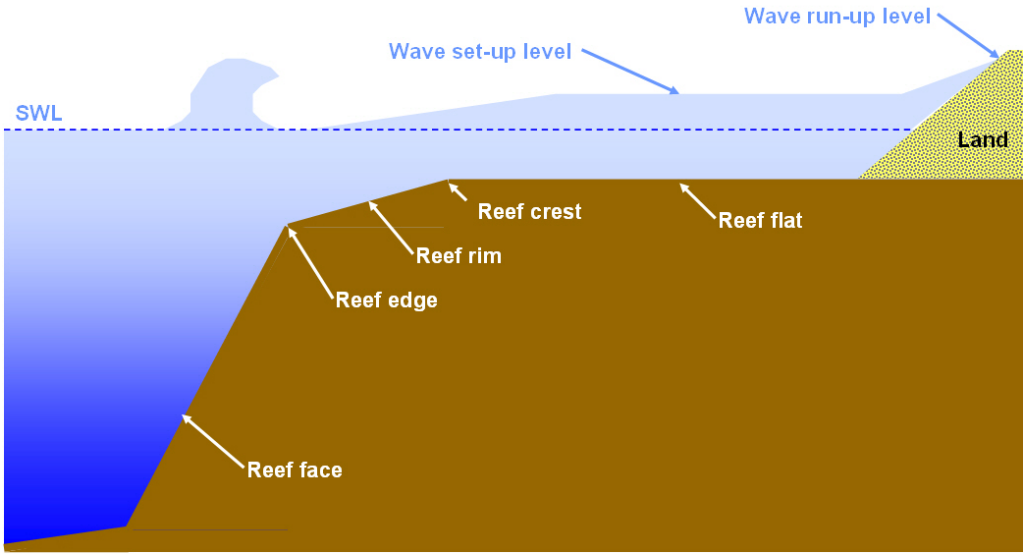


**Figure 24:** Fringing reef profile parameters as defined by Gourlay (1996, 1997) and as used in this report and the subsequent coastal calculator.

Taking these factors into account, the methodology suggested by Gourlay (1996, 1997) has been used to estimate wave set-up and the resulting height of waves translating over the ocean-side reef flat to the shoreline (see next section).

The range of wave conditions, water depths and reef characteristics makes it impractical to provide wave set-up values for every location in Kiribati, particularly as much of the local information, such as reef flat levels is not available. Instead a tool has been developed (the coastal calculator, see Section 9) to enable site-specific wave set-up, wave run-up and wave overtopping calculations to be made) using the extreme offshore significant wave heights described in the previous sections.

In terms of reef characteristics:

- The level of the reef, relative to the water level has the dominant influence on wave set-up magnitude. As the depth of water over the reef increases, the magnitude of wave set-up decreases (see Worked Example 1).

- The shape of the seaward reef profile also has a significant influence on mean wave set-up magnitude as it controls how waves break on the reef edge. Higher wave set-up occurs on steeper reef faces as wave breaking occurs over a narrower zone (see Worked Example 2).

**Worked example 1: Effect of water depth over the reef on wave set-up**

Conditions

| | |
|---|---|
| Offshore wave conditions: | Tarawa south coast: 1% AEP wave heights |
| Wave breaking location: | Reef edge and rim |
| Reef face slope: | 1:3 |
| Average reef flat levels: | 1.03 m, 1.53 m, 2.03 m, 2.53 m relative to SEAFRAME datum |
| Calculated storm tide level | 3.03 m relative to SEAFRAME datum |
| Resulting reef flat water depths: | 0.5 m, 1 m, 1.5 m, 2.0 m |

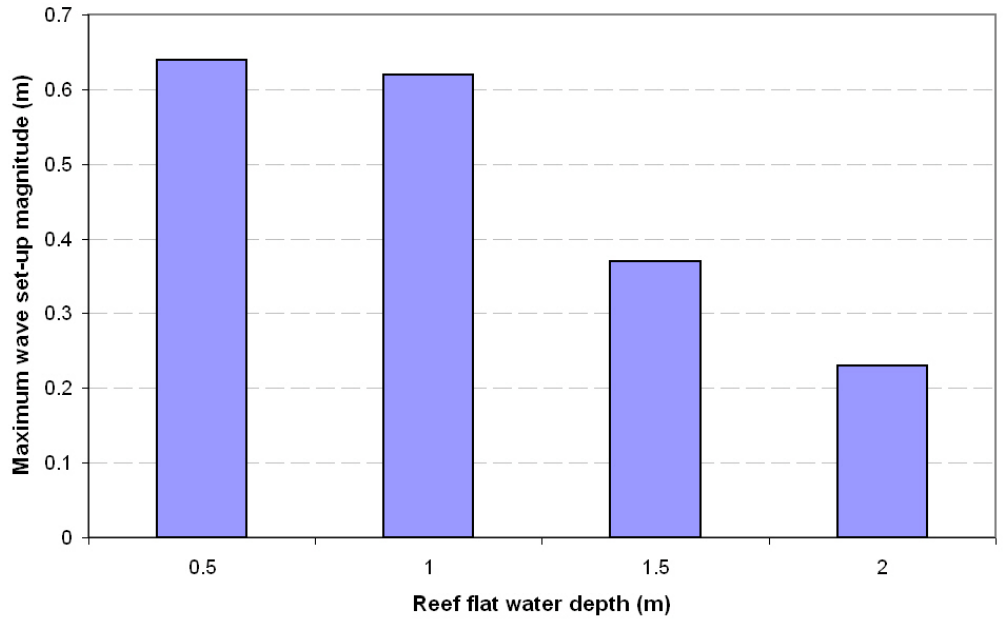


Figure description

The figure shows the maximum wave set-up magnitude, for this particular situation, for a range of water depths, from 0.5 m to 2.0 m for a 1% AEP offshore significant wave height.

Note: This figure cannot be created in the Coastal Calculator spreadsheet. The values of wave set-up for each water depth were calculated by the calculator and then plotted in a separate spreadsheet.

**Worked example 2: Effect of the slope of the reef on wave set-up**

Conditions

| | |
|---|---|
| Offshore wave conditions: | Tarawa south coast: 1% AEP wave heights |
| Wave breaking location: | Reef edge and rim |
| Reef face slope: | 1:1, 1:2, 1:3, 1:5, 1:10 |
| Average reef flat level: | 1.53 m, relative to SEAFRAME datum |
| Calculated storm tide level | 3.03 m relative to SEAFRAME datum |
| Resulting reef flat water depth: | 1 m |

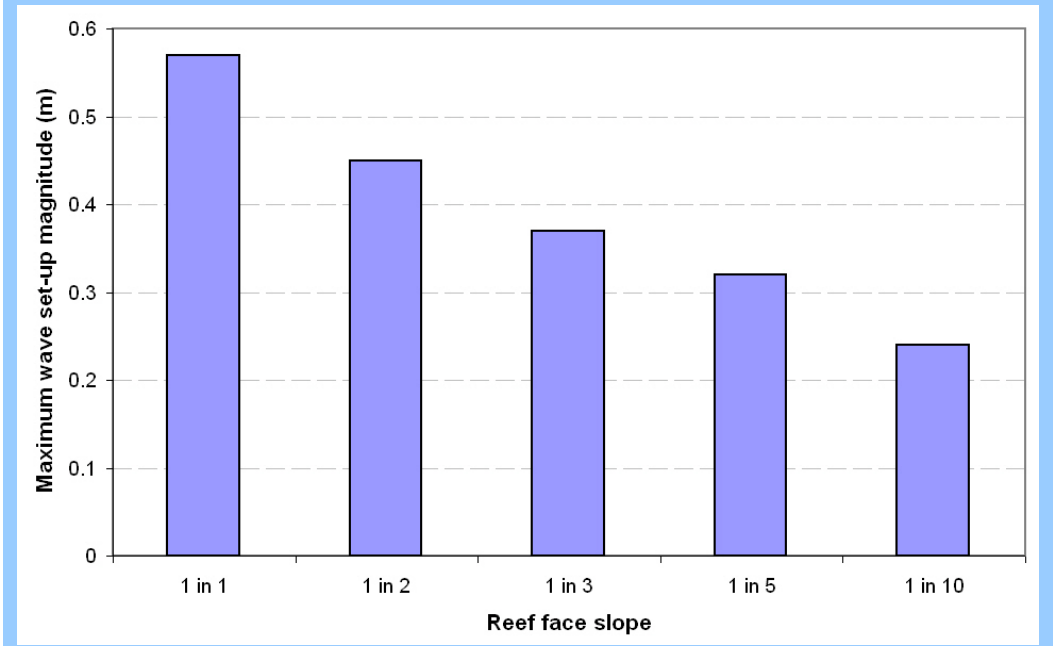


Figure description

The shape of the seaward reef profile also has a significant influence on wave set-up magnitude as it controls how waves break on the reef edge. The figure provides an example of how the magnitude of mean wave set-up can vary due to the slope of the reef face, with higher mean set-up occurring on steeper reef faces, caused by a narrower zone of wave breaking.

Note: This figure cannot be created in the Coastal Calculator spreadsheet. The values of wave set-up for each reef face slope were calculated by the calculator and then plotted in a separate spreadsheet.

### 5.2.2 Wave height translation over the ocean side fringing reef

The water depth over the reef flat also determines the size of the waves that can translate over the reef flat. As waves break on the edge of the reef, they reform into smaller waves, typically of shorter period, that are limited by the depth of water over the reef flat. The reformed waves behave as solitary waves, with the speed that they approach the shore being proportional to the water depth over the reef flat. When wave grouping results in increased water depth behind the crest of a wave, larger waves from behind travelling faster in the deeper water can overtake the wave in front. This situation can occasionally permit larger waves to reach the shore.

For practical purposes the method used for assessing wave height variation over the ocean side fringing reef flat is the method suggested by Gourlay (1996). This relates the wave height at any location on the reef flat to the total water depth (i.e., still water depth plus mean wave set-up), the offshore wave height, and a friction factor which depends on the characteristics of the surface of the reef flat. At the seaward edge of the reef, the maximum depth-limited wave height is approximately 40% of the total water depth over the reef (i.e., storm tide level plus wave set-up). The transformation of a breaking wave on the reef edge to a multi-crested system of shorter-period waves on the reef flat is based on the methodology of Galvin (1970) as presented in Gourlay (2007).

As with wave set-up, the Coastal Calculator (Section 9) has been developed to allow site-specific assessment of wave translation over an ocean-side fringing reef flat taking account of the particular offshore extreme wave conditions, water level over the reef flat, wave set-up, reef width and reef surface characteristics (Worked Example 3).

**Worked example 3: Example of the effect of wave height dissipation over a fringing reef flat due to different reef top characteristics**

Conditions

| | |
|---|---|
| Offshore wave conditions: | Tarawa south coast: 1% AEP wave heights |
| Wave breaking location: | Reef edge and rim |
| Reef face slope: | 1:3 |
| Average reef flat level: | 1.53 m, relative to SEAFRAME datum |
| Calculated storm tide level | 3.03 m relative to SEAFRAME datum |
| Resulting reef flat water depth: | 1 m |
| Reef flat width: | 200 m |
| Reef flat characteristics: | 75% - 100% sand |
| | 75%-100% smooth rock or coral pavement |
| | 25% - 50% live coral or dead un-eroded coral or tall (>30 cm boulders). |
| | 75% - 100% live coral or dead un-eroded coral or tall (>30 cm boulders). |

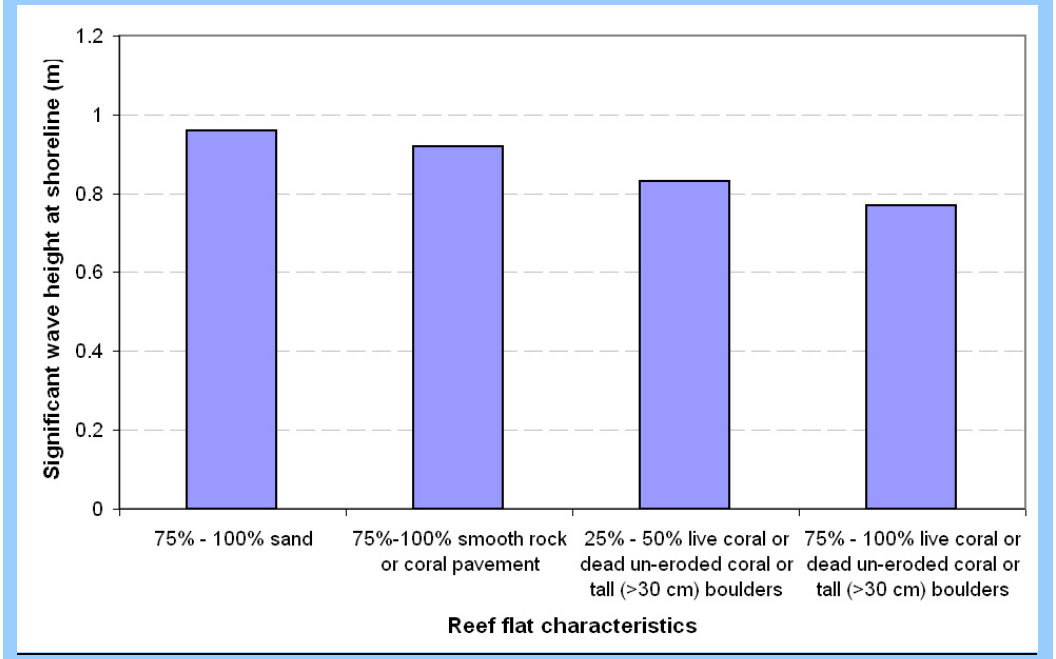


Figure description

The figure shows an example of the difference in wave height at the toe of the beach due to different reef flat characteristics. The smoother the reef flat, the less the dissipation of wave energy and hence higher waves reach the shoreline.

Removing coral rubble from reef flats for construction has been a common activity on many Pacific Islands with the result that larger waves reach the toe of the beach, resulting in an increase in erosion.

Note: This figure cannot be created in the Coastal Calculator spreadsheet. The values of wave height for different reef flat characteristics were calculated by the calculator and then plotted in a separate spreadsheet.

# 6. Wave conditions within Tarawa lagoon

## 6.1 Wave modelling

The information in Chapter 5 provided oceanic wave conditions in deep water offshore of the various atolls and islands in Kiribati. Wave conditions within Tarawa lagoon will be significantly influenced by both ocean swell and local wind-wave generation, and the dissipative effects of the much shallower lagoon seafloor. Where sufficiently detailed lagoon bathymetry is available, use can be made of a shallow-water wave model to simulate the effects of shallow-water processes on the wave climate as waves propagate towards the lagoon shoreline. For such modelling, sufficiently resolved lagoon bathymetry data are available for Tarawa lagoon only.

The nearshore wave model, SWAN (described in Appendix 3), was set up as follows:

- Firstly, a coarse model grid (resolution of 1000 m) was set up covering the Makin-Abaiang and Tarawa region (Figure 25, left). Nested within this coarse grid was a finer grid (100 m resolution) covering the Tarawa lagoon region (Figure 25, right).

- Multiple SWAN simulations were made using combinations of offshore significant wave height, peak wave period, peak wave direction, wind speed and direction, and water level. This forms the basis of a "lookup table" describing wave conditions inshore for a limited set of forcing conditions.

- Offshore boundary wave conditions were supplied from a time series of wave parameters from the Wavewatch III hindcast (discussed in Section 5) for the period 1 February 1997 to 1 November 2007. Time series were extracted from the four closest nodes to Tarawa (172.5°E 1°N, 172.5°E 2°N, 173.75°E 1°N, 173.75°E 2°N). These were merged into a single time series by using the node closest to the direction from which the waves approached Tarawa, so that the deep-water wave record was not compromised by shadowing from the Tarawa landmass.

- Through a process of multi-linear interpolations, a set of numerical weighted values were derived from the separate weightings for swell conditions, wind and tide height; with the latter being obtained from the SEAFRAME station. These weights were then used to enter the "lookup table", and compute wave values for each of the 23 output locations shown in Figure 25, for the present

day, and with sea-level rises of 0.48 m and 0.79 m (see Appendix 3, Section 13.2 for details).

An extreme analysis was conducted using the simulated time series of wave conditions at each of the 23 sites around Tarawa lagoon. Significant wave heights and peak wave periods corresponding to a range of annual exceedance probabilities (AEP) were computed for each of these 23 locations.

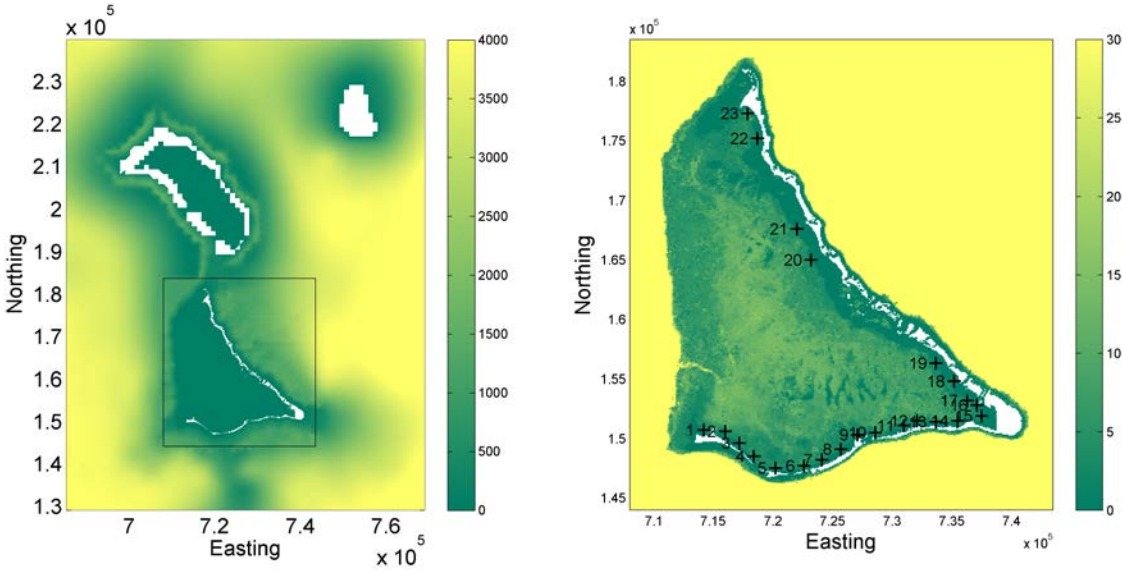


**Figure 25:** Extent of the coarse (left) and fine (right) model grid showing the ocean bathymetry used around Abaiang and Tarawa (right), and for Tarawa Lagoon (left). Depths are in metres.

## 6.2 Extreme wave heights in Tarawa lagoon

Figure 26 and Table 12 summarise the extreme wave heights at the 23 locations derived from the wave modelling within Tarawa lagoon for the present day, and for assumed sea-level rises of 0.48 m and 0.79 m. Note that the wave heights are not directly comparable for a particular AEP as the lagoon depth at each location varies, and that influences the wave height at any particular location. These wave conditions still need to be translated to the shoreline taking account of the effect of any back-reef flat or intertidal and sub tidal sand flats. This is discussed in Section 7.

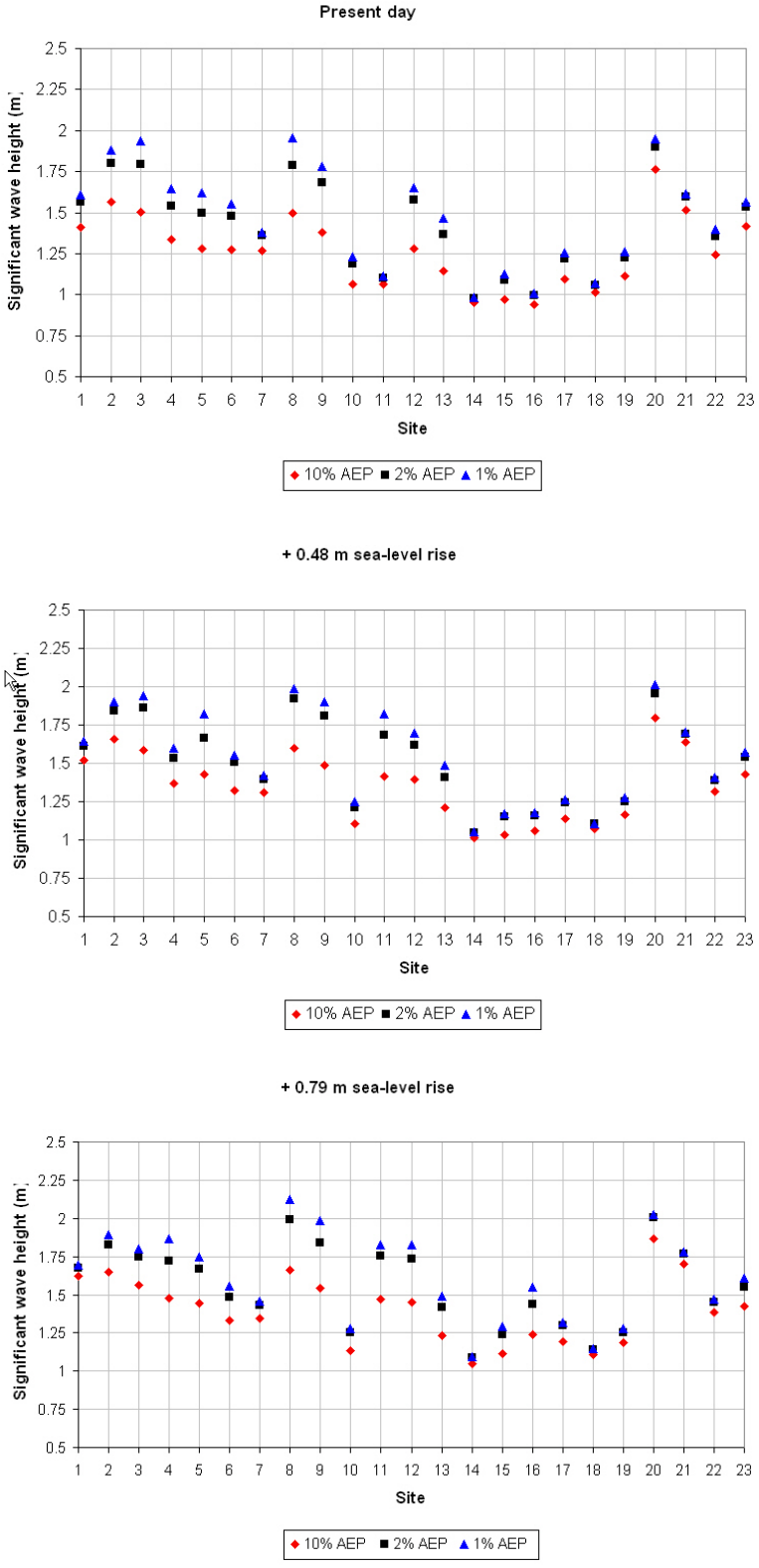


**Figure 26:** Predicted extreme wave heights at 23 sites within Tarawa lagoon for present-day sea level (top) and sea level rise scenarios of + 0.48 m (middle) and + 0.79 m (bottom).

**Table 12:** 10%, 2% and 1% annual exceedance probability (AEP) significant wave heights ($H_s$) at the 23 sites around Tarawa lagoon for the three sea-level rise scenarios: present day, +0.48 m and +0.79 m.

| Site | Location | Present day | | | + 0.48 m SLR | | | + 0.79 m SLR | | |
|---|---|---|---|---|---|---|---|---|---|---|
| | | 10% $H_s$ (m) | 2% $H_s$ (m) | 1% $H_s$ (m) | 10% $H_s$ (m) | 2% $H_s$ (m) | 1% $H_s$ (m) | 10% $H_s$ (m) | 2% $H_s$ (m) | 1% $H_s$ (m) |
| 1 | Betio (West) | 1.41 | 1.55 | 1.60 | 1.52 | 1.62 | 1.64 | 1.62 | 1.68 | 1.69 |
| 2 | Betio (Central) | 1.57 | 1.79 | 1.88 | 1.65 | 1.83 | 1.89 | 1.66 | 1.86 | 1.94 |
| 3 | Betio (East) | 1.49 | 1.76 | 1.87 | 1.56 | 1.78 | 1.87 | 1.55 | 1.75 | 1.83 |
| 4 | Causeway | 1.34 | 1.54 | 1.62 | 1.38 | 1.54 | 1.60 | 1.52 | 1.80 | 1.91 |
| 5 | Bairiki | 1.28 | 1.50 | 1.60 | 1.43 | 1.69 | 1.80 | 1.44 | 1.65 | 1.73 |
| 6 | Nanikai | 1.29 | 1.47 | 1.54 | 1.32 | 1.50 | 1.56 | 1.33 | 1.48 | 1.53 |
| 7 | Taeoraereke | 1.27 | 1.34 | 1.36 | 1.32 | 1.40 | 1.42 | 1.35 | 1.44 | 1.46 |
| 8 | Banraeaba | 1.49 | 1.76 | 1.88 | 1.60 | 1.90 | 2.03 | 1.66 | 1.98 | 2.11 |
| 9 | Taborio (West) | 1.40 | 1.67 | 1.78 | 1.50 | 1.79 | 1.91 | 1.56 | 1.86 | 1.98 |
| 10 | Taborio (East) | 1.07 | 1.19 | 1.23 | 1.11 | 1.22 | 1.26 | 1.13 | 1.23 | 1.27 |
| 11 | Eita (West) | 1.06 | 1.10 | 1.11 | 1.40 | 1.66 | 1.77 | 1.44 | 1.71 | 1.81 |
| 12 | Eita (Central) | 1.30 | 1.53 | 1.62 | 1.39 | 1.63 | 1.73 | 1.45 | 1.71 | 1.81 |
| 13 | Eita (East) | 1.15 | 1.34 | 1.42 | 1.21 | 1.40 | 1.47 | 1.25 | 1.43 | 1.50 |
| 14 | Bikenibeu | 0.95 | 0.98 | 0.98 | 1.02 | 1.05 | 1.05 | 1.05 | 1.09 | 1.09 |
| 15 | Bonriki | 0.97 | 1.07 | 1.11 | 1.03 | 1.14 | 1.17 | 1.12 | 1.25 | 1.30 |
| 16 | Buota (South) | 0.93 | 0.99 | 1.00 | 1.06 | 1.15 | 1.18 | 1.24 | 1.46 | 1.54 |
| 17 | Buota (North) | 1.09 | 1.21 | 1.25 | 1.15 | 1.25 | 1.28 | 1.19 | 1.29 | 1.32 |
| 18 | Abato | 1.01 | 1.07 | 1.08 | 1.07 | 1.10 | 1.11 | 1.11 | 1.14 | 1.14 |
| 19 | Tabiteuea | 1.12 | 1.22 | 1.25 | 1.17 | 1.25 | 1.27 | 1.19 | 1.26 | 1.27 |
| 20 | Abaokoro | 1.52 | 1.60 | 1.62 | 1.64 | 1.70 | 1.71 | 1.71 | 1.77 | 1.79 |
| 21 | Ereti | 1.77 | 1.92 | 1.96 | 1.80 | 1.95 | 2.00 | 1.85 | 2.00 | 2.04 |
| 22 | Tearinibai | 1.25 | 1.36 | 1.40 | 1.32 | 1.39 | 1.41 | 1.38 | 1.45 | 1.47 |
| 23 | Buariki | 1.40 | 1.52 | 1.56 | 1.43 | 1.55 | 1.59 | 1.43 | 1.56 | 1.60 |

# 7. Wave and storm tide joint probability conditions within Tarawa lagoon

## 7.1 Introduction

Run-up, overtopping and damage to structures located along atoll shorelines are usually associated with times when large waves *and* high sea levels coincide. When considering run-up, overtopping and inundation, or the design or hydraulic performance of coastal engineering structures, it is therefore important to consider both parameters together. The detailed analysis of extreme significant wave conditions (Section 6), and storm tide levels (Section 3) provides a basis to assess the joint occurrence (joint probability) of high waves and storm tide levels, i.e., how likely the two will occur simultaneously.

For each of the 23 locations around Tarawa lagoon for present day, and for sea-level rises of 0.48 m and 0.79 m, the ~33-year sea-level record (May 1974–Aug 2007) was used to describe the sea-level distribution and associated storm tide level predictions (described in Sections 3 and 4), while the 10-year wave hindcast was used to describe the wave height and period distribution and associated extreme wave height predictions (Section 6). Based on this, an objective joint probability assessment was made by matching the wave and sea-level records over the 10-year period, and using the matched records to extrapolate joint-probability contours for large return periods. A full description of the joint probability methodology is provided in Appendix 3 (Section 13.3).

Following this report being finalised joint probability conditions were also derived for the south, north (east) and west ocean coastlines of Tarawa and are included in Appendix 6.

## 7.2 Joint probability combinations

Joint probability combinations of wave height and storm tide levels for each of the 23 lagoon and 3 ocean locations have been derived for annual exceedance probabilities (AEP) between 10% (approximately 10 year return period) and 1% (100 year return period). Figure 27 shows an example of the various wave height and storm tide level contours for Site 1 at western Betio under present-day conditions (black lines) and assuming sea-level rises of +0.48 m (blue lines) and +0.79m (red lines). Any combination of storm tide level and wave height lying along a given contour line has an equal probability of occurring (or the same average return period).

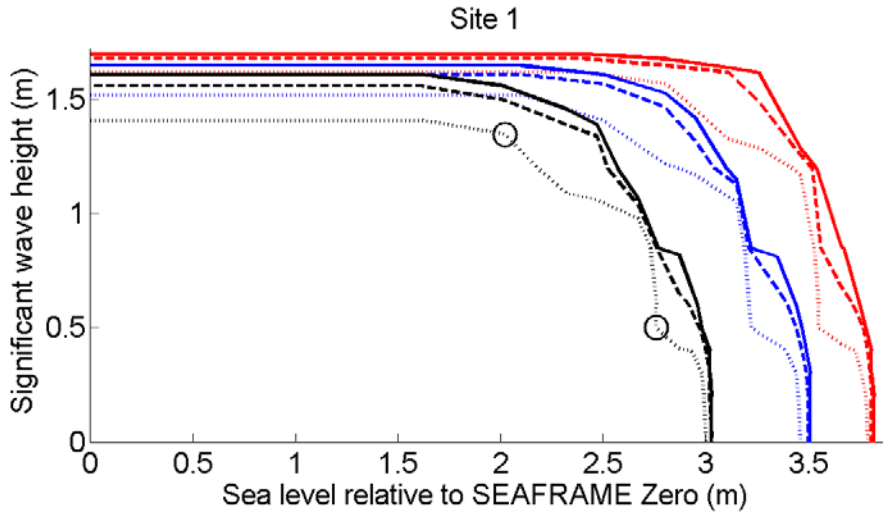


**Figure 27:** Joint probability results for Site 1 at western Betio. The black lines mark the wave and storm tide level contours for a 10% AEP (dotted line), 2% AEP (dashed line) and 1% AEP (solid line) for present-day sea levels. The blue lines are for +0.48 m sea-level rise, and the red lines are for +0.79 m sea-level rise.

For example, in Figure 27 the two circles mark storm tide/wave height combinations for present day sea levels of 2.02/1.35 m and 2.76/0.5 m, both of which have a 10% probability of being equalled or exceeded during any given year.

Figure 27 also shows the joint probability contours for 10%, 2% and 1% AEP combinations for Site 1, associated with rises in mean level of the sea of +0.48 m (blue lines) and +0.79 m (red lines). This results in the wave/storm tide level joint probability shifting up and to the right, reflecting more commonly occurring combined storm tide levels and waves. Appendix 6 contains all the joint probability plots and tables for all 23 sites for the present day and for sea-level rises of 0.48 m and 0.79 m, and for the three ocean shorelines for Tarawa.

The 23 lagoon locations where the storm tide, extreme significant wave heights and the resulting joint probability combinations have been calculated tend to be just seaward of any back reef or sub/intertidal flats. To transfer these combinations of conditions at the shoreline (for wave run-up and overtopping calculations) the following was conducted:

- For a defined back reef such as found along the southern lagoon coastline of Tarawa, wave set-up and wave height translation over the back reef flat are calculated in the same way as for the ocean-side reef flat (described in Section 5.2). Given the smaller wave heights, shorter wave periods and width of reef

flat, any wave set-up due to wave breaking on the lagoon edges of any back reef is likely to be minimal.

- For the majority of the lagoon shoreline, which slopes gently towards the lagoon, shallow-water effects on wave conditions were accommodated using a simple empirical relationship that takes account of parameters such as wave height, period and the slope of the lagoon bed to calculate wave conditions at the shoreline (Goda, 1980).

- In such situations, any wave set-up occurs inshore of where waves are breaking and is likely to be low.

# 8. Wave run-up and overtopping

## 8.1 Introduction

Wave run-up and overtopping of coastal defences can be highly variable and site specific, depending on factors such as wave height and period, beach or defence slope and profile, and the nature of the beach or defence (i.e., the roughness). The range of combinations resulting from offshore (or lagoon) wave and sea level conditions, reef flat and shoreline characteristics make it difficult to provide generalised results of wave run-up levels and overtopping discharge. Instead a spreadsheet-based calculator has been developed as part of this project to allow calculations of wave run-up levels and overtopping rates to be made for site-specific locations using the wave and sea level information described in the previous sections of this report (Section 9). Outlined below is a brief description of the methodologies used within the calculator to derive values for wave run-up and overtopping.

## 8.2 Wave run-up

Run-up is defined as an elevation above the reef flat sea level (i.e., for reef environments the total sea level combining the tide, any storm surge and wave set-up over the reef flat). Run-up level varies on a wave-by wave basis and for practical purposes is normally defined as the level exceeded by 2% of the run-up.

### 8.2.1 Wave run-up on beaches

Most empirical relationships for wave run-up have been derived for continental coastlines and relate run-up level to offshore wave conditions (wave height and period or wave length) and the slope of the beach, assuming a plane slope. There have been very few studies of wave run-up on fringing reef coastlines and little guidance on empirical relationships for calculating wave run-up in such locations. Initially three run-up methods were adopted (Holman, 1986; Stockdon et al. 2006; Gourlay, 1997). However, based on visual observations during two events where run-up was significant on the south coast of Tarawa after this report was finalised, these were found to under predict. Further empirical methods were subsequently assessed including Mase (1989), Hedges & Mase (2004) and Seelig (1983). The approach used by Mase (1989) along with use of the deep water wave length and maximum value of wave set-up was subsequently adopted which provided wave run-up levels close to those observed during the events:

$$R_{u2\%} = 1.86 H_r \xi^{0.71}$$

and

$$R_{\max} = 2.32 H_r \xi^{0.77}$$

Where:

$R_{u2\%}$ is the run-up level exceeded by 2% of the waves

$H_r$ is the significant wave height at the toe of the beach

$\zeta$ is the Iribarren number, which is: $\frac{\beta}{\left(H_r / L_r\right)^{0.5}}$ .

$L_r$ is the offshore wave length

$T_r$ is the mean wave period over the reef flat,

$\beta$ is the beach slope,

For coral rubble beaches (with a size of coral rubble < 0.1 m) where the profile can adjust to changing wave conditions, the crest elevation will change so that only the highest waves will overtop the beach crest. The height of the beach crest is typically approximately close to the 2% run-up level. Pullen et al. (2007) provide a relationship which has been adjusted for the depth-limited reef environment to:

$$h_c = 0.3 H_r s^{-0.5}$$

where $h_c$ is the height of the beach crest above the mean water level, $H_r$ is the wave height at the toe of the beach and s is the wave steepness over the reef.

### 8.2.2 Wave run-up on sloping coastal defence structures

For run-up on sloping coastal defence structures, the relationship provided by Pullen et al. (2007) is used, again adjusted for depth-limited wave conditions over the reef flat:

$$R_{u2\%} = 1.65 H_r \gamma_f \zeta_r$$

The maximum value is:

$$R_{u2\%} = H_r \gamma_f \left( 4.0 - \frac{1.5}{\sqrt{\zeta_r}} \right)$$

where $\gamma_f$ is a factor depending on the permeability and roughness of the slope of the structure, with the other parameters as above. Wave run-up can also depend on the angle that waves approach the shoreline. In this study, we have assumed that all waves approach the shoreline parallel to the shoreline or defence structure which is the worst case for overtopping.

## 8.3 Wave overtopping of coastal defence structures

Wave overtopping of a structure can occur in a number of ways (HR Wallingford, 1999). "Green water" overtopping occurs as a result of waves running up the face of a coastal structure. If run-up levels are high enough, water will pass over the crest of the structure (Figure 28, left). A second form is where waves break directly on to the seaward face of the structure and produce significant volumes of splash (Figure 28, right). This splash may be then carried over the crest of the structure either under its own momentum, or as a consequence of associated strong onshore winds. Wave overtopping can also be caused by spray due to the action of the wind on wave crests immediately offshore of the structure.

Existing empirical formulae for predicting overtopping rates typically include the green water and splash components but do not include wind spray. However, wind spray typically only influences overtopping rates when the rates of green water and splash are low; under higher green water rates the impact of spray is minimal on the total rate.

**Figure 28:** Wave run-up and overtopping of a sloping revetment (right) and overtopping of a vertical wall due to wave breaking on to the wall (right).

The mean rate of water overtopping[3] is calculated based on the empirical approaches summarised in *Wave overtopping of seawalls: Design and assessment manual* (HR Wallingford, 1999), and *EurOtop: Wave overtopping of sea defences and related structures: Assessment Manual* (Pullen et al. 2007). Overtopping assessment, using the calculator (Section 9), is available for three basic types of coastal defence:

- Sloping (i.e., revetment) seawalls, with varying slopes between 1 in 1 to 1 in 5, and different types of coastal defence armouring.
- Plane vertical walls.
- Composite vertical walls (vertical walls with toe protection).

Overtopping rates are very sensitive to small variations in coastal defence geometry, local bathymetry and wave conditions reaching the toe of the structure. In general, it is reasonable to assume that the overtopping rates predicted by the different approaches are accurate to an order of magnitude and give a reasonable indication of the magnitude of change in overtopping and frequency, relative to the present, that could occur in the future due to climate change effects.

In general wave run-up and overtopping of a structure depend on:

- Wave height: the larger the waves at the toe of the defence the larger the run-up and overtopping rate.

[3] Mean overtopping rate or discharge is typically expressed in litres per second per metre length of defence (l/s/m) or cubic metres per second per metre length of defence ($m^3$/s/m). To convert $m^3$/s/m to l/s/m divide $m^3$/s/m by 1000.

- Wave period: the larger the wave period the higher the run-up and overtopping rate.

- Defence slope: the steeper a slope (for a revetment), the higher the run-up and overtopping rate.

- Defence armour: an impermeable and smooth armour layer will have higher run-up and overtopping than a permeable and rough armour layer.

- Crest height: the lower the crest the higher the overtopping rate.

- Crest width: the narrower the crest of the defence the higher the overtopping rate (only for defences where the armour layer is porous, e.g., rock rip-rap, gabions).

There are also a number of other design features that can be used to reduce overtopping rates, such as berms within the slope of a revetment, and wave crest or return walls at the crest of the structure. Overtopping rate also depends on the angle that waves approach the shoreline, but for this study we have assumed that all waves approach parallel to the shoreline.

### 8.3.1 Tolerable overtopping discharges

Damage to coastal defences, infrastructure or buildings located behind such structures and the risks to people due to wave overtopping have traditionally been given as a function of mean overtopping discharge. Typically overtopping limits are related to mean overtopping rates but it is well known that it is peak overtopping volumes that initiate or cause damage. However, much less is known about peak overtopping damage thresholds (Pullen et al. 2007). Table 12 provides some general guidance on mean wave overtopping limits.

**Table 12:** Tolerable limits of mean wave overtopping.

| Hazard type | Mean overtopping rate (l/s/m) | Mean overtopping rate ($m^3$/s/m) |
|---|---|---|
| Public: Aware public, clear view of the sea, not easily upset or frightened, able to tolerate getting wet | 0.1 | 0.00001 |
| Vehicles: Driving at low speeds, overtopping at low flow depths | 10 – 50* | 0.01-0.05 |
| Damage to buildings | 1 | 0.001 |
| Damage to unprotected area behind seawall | 50 | 0.05 |
| Damage to paved or armoured area behind seawall | 200 | 0.2 |

* Set as 30 l/s/m in the Coastal Calculator

# 9. An overview of the coastal calculator

## 9.1 Introduction

The Coastal Calculator was developed to aid the use and application of coastal data and information derived within the *Climate Information for Risk Management* component of KAP II. Its purpose is to:

1. Act as a database for:
    - Extreme offshore significant wave heights around each island in Kiribati and at 23 locations around the Tarawa lagoon shoreline.
    - Extreme storm tides at 23 locations around the Tarawa Lagoon shoreline and for Tarawa ocean shoreline.
    - Joint occurrence of extreme wave heights and storm tide levels at 23 locations around Tarawa lagoon shoreline, and off the north (east), south and west Tarawa ocean coasts.
    - Annual Mean Level of the Sea (MLOS) data from the University of Hawaii and SEAFRAME tide gauges from 1974 to present.
    - Sea-level rise (5%, central estimates and 95% range) for the six emission scenarios used by the IPCC AR4 and allowance for additional ice sheet discharge based on IPCC AR4 guidance.
2. Enables site specific calculations to be made, and comparison between, present day and potential future (based on defined climate change scenarios and timeframes) values of:
    - Mean and high tide levels.
    - 10%, 2%, 1% Annual Exceedance Probability (AEP) conditions for:
        - Storm tide levels.
        - Wave set-up levels over the fringing reef flat (on ocean shoreline).
        - Wave heights at the shoreline.
        - Wave run-up levels on beaches or sloping seawalls.
        - Wave overtopping volumes for a range of different seawall types.

The coastal calculator provides information to support assessments of how inundation potential may change under different climate change scenarios and future timeframes. It does not assess inundation directly, rather provides information on the "drivers" of inundation (waves and water levels at the shoreline, wave run-up and overtopping) and how these will change over this century due to climate change impacts.

Its main use will be to assist climate change risk assessments associated with:

- Climate proofing land and development planning :
    - Assessing areas at potential risk from inundation (both in terms of frequent events, e.g., high tides, to less frequent storm-related events) and how these may change.
    - Setting minimum ground levels or floor levels for development activities.
    - Establishing the extent of existing building inundation risk and how this may change in the future.
- Coastal engineering:
    - Deriving seawall design wave / water level conditions that account for climate change effects.
    - Assessing adequacy of the design of seawall permit applications.
    - Basic seawall profile design optimisation (to optimise performance in reducing wave overtopping).
    - Basic assessments of how overtopping of existing seawall structures may change and how these relate to dangerous overtopping limits.

The methodologies used to derive the data held in the calculator, and the calculations carried out by the calculator are described in the various sections earlier in this report.

Full details of the Coastal Calculator, its use, and a number of worked case examples are provided in the supporting Operational Handbook (Ramsay, 2010).

# 10. References

AMSAT, AusAID, NTF Australia (2004). Pacific country report on sea level and climate: their present state. Kiribati. June 2002. Australian Agency for International Development. Australian Marine Science and Technology Limited. National Tidal Facility Australia, JC0163a, 19 p.

Andersen, O.B.; Egbert, G.D.; Erofeeva, S.Y.; Ray, R.D. (2006). Mapping nonlinear shallow-water tides: a look at the past and future. *Ocean Dynamics 56(5).* Pp.416-429.

Bamber, J.L.; Alley, R.B.; Joughin, I. (2007). Rapid response of modern day ice sheets to external forcing. *Earth and Planetary Science Letters 257*: 1-13.

Booij, N.; Ris, R.C.; Holthuijsen, L.H. (1999). A third-generation wave model for coastal regions, Part I, Model description and validation. *Journal of Geophysical Research 104*: 7649-7666.

Bureau of Meteorology (2008). Pacific country report. Sea level and climate: Their present state. Kiribati, December 2008.

Coles, S. (2001). An introduction to statistical modelling of extreme values. Springer. London; New York.

Goda, Y. (1980). Randon seas and design of maritime structures. University of Tokyo Press.

Galvin, C.J. (1970). Finite-amplitude, shallow water-waves of periodically recurring form. In Proc. Symposium of Long Waves, University of Delaware. US Army Corps of Engineering Coastal Engineering Research Centre Reprint 5-72.

Global Carbon Project (2008). Growth in the global carbon budget. Press release, 25 September 2008. http://www.globalcarbonproject.org/carbontrends/index.htm. Accessed 26 September 2008.

Grinsted, A.; Moore, J.C.; Jevrejeva, S. (2010). Reconstructing sea level from paleo and projected temperatures 200 to 2100 AD. *Climate Dynamics* 34: 461-472.

Gourlay, M.R. (1996). Wave set-up on coral reefs. 2. Set-up on reefs with various profiles. *Coastal Engineering 28*: 17 – 55.

Gourlay, M.R. (1997). Wave set-up on coral reefs: Some practical examples. Paper presented at the Combined Australasian Coastal Engineering and Ports Conference, Christchurch, 1997. Pp. 959-964.

Government of Kiribati (2005). Climate Change Adaptation (CCA) Strategy, June 2005.

Hedges, T.S.; Mase, H. (2004). Modified Hunt's equation incorporating wave setup. *Journal of Waterway, Port, Coastal and Ocean Engineering 130(3)*: 109-113.

Holman, R.A. (1986). Extreme value statistics for wave run-up on a natural beach. *Coastal Engineering 22(1)*: 81-92.

Horton, R.; Herweijer, C.; Rosenzweig, C.; Liu, J.; Gornitz, V. & Ruane, A.C. (2008). Sea level rise projections for current generation CGCMs based on the semi-empirical method, *Geophys. Res. Lett. 35*, L02715, doi:10.1029/2007GL032486.

Wallingford, H.R. & Lancaster University (2000). The joint probability of waves and water levels: JOIN-SEA, a rigorous but practical new approach. HR Wallingford Report SR 537.

Wallingford, H.R. (1999). Overtopping of seawalls. Design and assessment manual. Environment Agency R & D Technical Report W178.

Jevrejeva, S.; Moore, J.C.; Grinsted, A. (2010). How will sea level respond to changes in natural and anthropogenic forcings by 2100? *Geophys. Res. Lett. 37*, L07703 doi:10.1029/2010GLA042947.

Mase, H. (1989). Random wave run-up height on gentle slope. *Journal of Waterway, Port, Coastal and Ocean Engineering 115(5)*: 649-661.

Matthews, L.S. (1971). Heavy swell observed in the South Pacific in December 1969. New Zealand Meteorological Service. Technical Note 196, 11 pp.

National Tidal Centre (2007). The South Pacific sea level and climate monitoring project. Monthly data report 50. December 2007.

Pawlowicz, R.; Beardsley, B.; Lentz, S. (2002). Classical tidal harmonic analysis including error estimates in MATLAB using T_TIDE. *Computers and Geosciences 28*: 929-937.

Pfeffer, W.R.; Harper, J.T.; Neel, S.O. (2008). Kinematic constraints on glacier contributions to 21st-century sea-level rise. *Science 321*: 1340-1343.

Pullen, T.; Allsop, N.W.H.; Bruce, T.; Kortenhaus, A.; Schüttrumpf, H.; Van der Meer, J.W. (2007). EurOtop: wave overtopping of sea defences and related structures: Assessment Manual. August 2007. Available from www.overtopping-manual.com

Rahmstorf, S. (2007). A semi-empirical approach to projecting future sea level rise, *Science 315*: 368–370.

Ramsay, D.L. (2010). Kiribati Adaptation Project Phase II: Climate Information for Risk Management. Coastal calculator operational handbook. NIWA Client Report: HAM2009:165, April 2010.

Rignot E.; Bamber J.L.; van der Broeke, M.R.; Davis, C.; Li, Y.; Van der Berg, W.J.; Van Meijgaard, E. (2008). Recent Antarctic ice mass loss from radar interferometry and regional climate modelling. *Nature Geoscience 1*: 106–110.

Ris, R.C.; Holthuijsen, L.H.; Booij, N. (1999). A third-generation wave model for coastal regions - 2. Verification. *Journal of Geophysical Research-Oceans 104*: 7667-7681

Seelig, W.N. (1983). Laboratory study of reef-lagoon systems hydraulics. *Journal of Waterway, Port, Coastal and Ocean Engineering 109(4)*: 380-391.

Shepherd, A.; Wingham, D. (2007). Recent sea-level contributions of the Antarctic and Greenland ice sheets. *Science 315*: 1529–1532.

Stephens, S.A.; Gorman, R.M. (2006). Extreme wave predictions around New Zealand from hindcast data. *New Zealand Journal of Marine and Freshwater Research 40*: 399-411.

Stockdon, H.F.; Holman, R.A.; Howd, P.A.; Sallenger, A.H. (2006). Empirical paramterization of setup, swash and run-up. *Coastal Engineering 53*. Pp. 573-588.

Thompson, C.; Mullan, B.; Burgess, S.; Ramsay, D. (2008). Kiribati Adaptation Programme. Phase II: Information for Climate Risk Management. High intensity rainfall and drought, NIWA Consulting Report to Government of Kiribati, WLG2008-12, 83 p.

Tolman, H.L. (1999). User manual and system documentation of WAVEWATCH-III Version 1.18, NOAA / NWS / NCEP / OMB. 110 p.

Tolman, H.L.; Balasubramaniyan, M.; Burroughs, L.D.; Chalikov, D.V.; Chao, Y.Y.; Chen, H.S.; Gerald, V.M. (2002). Development and implementation of wind-generated ocean surface wave models at NCEP. *Weather and Forecasting 17(2)*: 311–333.

Vermeer, M.; Rahmstorf, S. (2009). Global sea level linked to global temperature change. *Proc. Natl. Sci. U.S.A. 106(51),* doi: 10.1073/pnas.0907765106.